THE ASTROPHYSICAL JOURNAL SUPPLEMENT SERIES, 79:105–121, 1992 March

SHORT- AND INTERMEDIATE-PERIOD OXYGEN-RICH MIRAS

M. JURA
Department of Astronomy, University of California, Los Angeles, CA 90024
AND
S. G. KLEINMANN
Department of Physics and Astronomy, University of Massachusetts, Amherst, MA 01003
Received 1991 May 9; accepted 1991 August 28

ABSTRACT

Using available infrared photometry and the period-infrared luminosity relationship, we have analyzed a nearly complete sample of oxygen-rich Miras at Galactic latitudes with $|b| > 30°$. In agreement with previous kinematic studies, we find a marked difference in the spatial distributions between the stars with periods less than and those with periods greater than 300 days. For the stars with $300 < P < 400$ days (our "intermediate"-period Miras), the exponential scale height from the Galactic plane is close to 240 pc, the projected surface density is ~ 100 kpc^{-2}, and the local space density is ~ 210 kpc^{-3}. Those stars with periods less than 300 days (our "short"-period Miras) can have their distance from the Galactic plane modeled by an exponential with a scale height of between 500 and 600 pc, depending upon the zero point of the period-luminosity relationship, which is probably metallicity dependent. These short-period Miras do not belong to the standard "thin disk" population which has a maximum exponential scale height of ~ 300 pc. The surface density projected onto the Galactic plane of these short-period Miras is between 40 and 60 kpc^{-2}, and the space density in the Galactic plane is between 35 and 60 kpc^{-3}.

The progenitors of the Miras with $P > 300$ days appear to be disk dwarfs with typical main-sequence masses of between 1.0 and 1.2 $M_\odot$. The masses of the main-sequence progenitors of the short-period Miras are 1.1 $M_\odot$ or less. A typical mass for the main-sequence progenitors of less than 1 $M_\odot$ would indicate an age greater than 10^{10} yr for these stars; this result would pose a severe difficulty for understanding the white dwarf luminosity function since it would produce many more old white dwarfs with luminosities of less than 10^{-4} $L_\odot$ than are observed. Because they exhibit significant amounts of circumstellar dust, we estimate that the metallicity of the short-period Miras is at least one-third of the standard solar value.

We estimate a duration of the Mira phase for the intermediate-period stars to be $\sim 2 \times 10^5$ yr, somewhat longer than other recent estimates. Both short- and intermediate-period oxygen-rich Miras characteristically lose mass at $\sim 10^{-7}$ $M_\odot$ yr^{-1}.

Subject headings: stars: evolution — stars: kinematics — stars: variables: long-period variables

1. INTRODUCTION

Using the available infrared surveys, we are undertaking a systematic survey of bright, cool stars. Previously, we have discussed carbon stars (Claussen et al. 1987), S-type stars (Jura 1988), all AGB stars losing mass at rates greater than $\sim 2 \times 10^{-6}$ $M_\odot$ yr^{-1} (Jura & Kleinmann 1989) within 1 kpc of the Sun, the carbon stars losing large amounts of mass between 1 and 2.5 kpc from the Sun (Jura & Kleinmann 1990a), and very luminous ($L > 10^5$ $L_\odot$) supergiants (Jura & Kleinmann 1990b). Here, we consider the space distribution and evolutionary status of short- and intermediate-period oxygen-rich Miras.

Main-sequence stars with masses less than ~ 5 $M_\odot$ evolve to white dwarfs of perhaps 0.6 $M_\odot$ (see the review by Weidemann 1990). Some of this mass loss occurs during the Mira phase (see the review by Habing 1990) when the stars are on the asymptotic giant branch and have luminosities near 10^4 $L_\odot$. Because Miras are very luminous, they can be observed at great distances from the Sun. Therefore, they can be used to probe both the structure of the Milky Way including the bulge (Whitelock, Feast, & Catchpole 1991), and the Magellanic Clouds (Hughes & Wood 1990).

Most previous studies of Miras have tended to rely upon optical data to determine distances (see, for example, Sivagnanam, Le Squeren, & Foy 1988), but infrared data are more suitable. First, Miras are cool and emit most of their energy in the infrared. Also, their amplitudes of variability are markedly less at infrared than at optical wavelengths (see, for example, Lockwood & Wing 1971). Finally, the corrections for interstellar and circumstellar extinction are much less important at infrared compared to optical wavelengths. The period–K band luminosity relationship for Miras in the period range 100–400 days is well established (Feast et al. 1989; Reid, Glass, & Catchpole 1988), and therefore it is possible to estimate distances to individual Miras with some confidence.

Even previous studies of Miras which have used infrared data to estimate distances have suffered from incompleteness. Wyatt & Cahn (1983) analyzed a sample of Miras for which radial velocities and proper motions were available; they were selected on the basis of being optically bright. With the availability of the infrared surveys, it is possible to study systematically the entire sky at wavelengths optimized for Miras. We also can use the *IRAS* data to estimate the mass-loss rate from stars (see, for example, Jura 1990).

One goal of this paper is to develop a better understanding of the spatial distribution of oxygen-rich Miras in the neighborhood of the Sun. Previously, Wood & Cahn (1977) proposed an exponential scale height for Miras of 310 pc, while Wyatt & Cahn (1983) derived a value of more than 400 pc and Sivagnanam et al. (1988) used a value of 700 pc. With the available infrared data, it is possible to make sufficiently accurate statistical estimates of the distances to distinguish among these possibilities.

Feast (1963) has noted that Miras of different periods exhibit distinctive kinematic properties; the shorter the period the greater the space velocity. As reviewed by Plaut (1965), the dispersion of the velocity perpendicular to the Galactic plane for the stars with periods less than $\sim$300 days is near 55 km s^{-1}, about twice the mean dispersion of stars with periods longer than 300 days which is $\sim$28 km s^{-1}. Little, Little-Marenin, & Bauer (1987) have found that oxygen-rich Miras with periods greater than 300 days display Tc in their optical spectra while the Miras with periods less than 300 days do not show Tc, and therefore, it seems that one natural break in the properties of Miras is at 300 days. Feast (1989) has noted that the short-period Miras can be used to probe the structure of the putative "thick disk."

Habing (1988) has modeled the spatial distribution of the sources in the *IRAS* Point Source Catalog (1985) with $0.82 < F_\nu(25\ \mu m)/F_\nu(12\ \mu m) < 3.8$. while Harmon & Gilmore (1988) have modeled the spatial distribution of the *IRAS* sources with $0.625 < F_\nu(25\ \mu m)/F_\nu(12\ \mu m) < 2.5$ and 1 Jy $< F_\nu(12\ \mu m) < 8$ Jy. Most Miras are less red and are losing less mass than these other stars.

Miras evolve into white dwarfs. As a result, the space distribution of Miras can be used to estimate the density and luminosity functions of white dwarfs, and the luminosity function of white dwarfs has been used to estimate the age of the Galactic disk. Winget et al. (1987) and Liebert, Dahn, & Monet (1988) have found a sharp drop in the luminosity function of white dwarfs for $L < 10^{-4}\ L_\odot$. They explain this sharp drop as indicating that the age of the Galactic disk is $\sim$8 billion yr, because if there were older white dwarfs present they would have cooled to lower luminosity than what is observed. Iben & Tutukov (1984) have noted that a lack of very old, low-luminosity white dwarfs might be partly explained if such stars display a much greater mean distance from the Galactic plane than do the younger, higher luminosity white dwarfs. Here, we hope to evaluate this proposal quantitatively by determining the spatial distribution of the different populations of Miras.

In § 2, we describe our sample of stars and our method for determining their distances. In § 3, because there is a large amount of infrared and radio data, we first derive the properties of the intermediate-period ($300 < P < 400$ days) Miras, while in § 4, we consider the short-period ($P < 300$ days) oxygen-rich Miras. Because there are only 20 of them in our search zone, we do not analyze in detail the Miras with $P > 400$ days. In § 5, we discuss the implications of our results, and in § 6, we present our conclusions.

2. THE SAMPLE OF STARS

We first survey two cones at Galactic latitudes with $|b| \geq 30°$, because in this region of the sky (1) we expect less than 1.0 mag of optical absorption, and (2) we can avoid large-scale nearby features like Gould's Belt, and almost all of the local dark clouds (Lynds 1962) and molecular material (Magnani, Lada, & Blitz 1986). Since Miras are conspicuous by their long periods, large amplitudes of optical variations, and red colors, and since the sky has been scanned optically for centuries, we expect that most Miras at high latitude are cataloged in the General Catalog of Variable Stars (Kholopov et al. 1985, hereafter GCVS). In Appendix A we discuss the completeness of the sample of Miras. We argue that we have identified more than 90% of the high-latitude, intermediate-period Miras within 1300 pc of the Sun and more than 75% of all the high-latitude, short-period Miras within 2000 pc of the Sun.

According to the GCVS, Mira variables have $P \geq 80$ days and amplitudes at visual or blue wavelengths, $\Delta m, \geq 2.5$ mag. We adopt these criteria as necessary and sufficient conditions for the designation of a star as a Mira variable, in contrast to the GCVS, which lists some stars with such long periods and large amplitudes as semiregular. We assume that all of the stars in our sample are oxygen-rich unless classified otherwise, since the majority of classified Miras are oxygen-rich.

Tables 1 and 2 list all stars with $|b| \geq 30°$, and $\Delta m \geq 2.5$ mag, in two period ranges: Table 1 lists 107 with $300 \leq P \leq 400$ days while Table 2 lists 211 with $P \leq 300$ days. Over 90% of these stars were identified as Miras in the GCVS; the others were designated semiregulars. We also list the parameter, f, which characterizes the asymmetry of the optical light curve; we discuss the importance of this parameter in Appendix B. We omit XY Tau from Table 2, even though it meets our criteria for inclusion, because upon further study it is not a Mira variable (Whitelock et al. 1991b).

A histogram of the observed light excursions for the stars in Tables 1 and 2 is shown in Figure 1. It is evident that most of the stars in the sample display substantially greater variations than the minimum of 2.5 mag. Thus, this is a robust selection criterion.

The most accurate method to determine the distance to Miras is from the infrared period-luminosity relationship. For the Magellanic Cloud stars, Feast et al. (1989) proposed that:

$$M_K = -3.47 \log (P) + 1.01 , \quad (1)$$

where P is the period measured in days and M_K is the mean of the maximum and minimum absolute K magnitude. Because of the different metallicities between the stars in the LMC and those in the local Milky Way, Wood (1990) has extrapolated from pulsation theory to argue that the local stars are intrinsically fainter at K by 0.25 mag and therefore

$$M_K = -3.47 \log (P) + 1.26 . \quad (2)$$

In this paper we adopt equation (2) instead of equation (1) even though the result is based on theory which is not, at least yet, observationally confirmed (see Feast et al. 1989). This factor of 0.25 mag corresponds to a difference of 12% in the derived distance. In all cases, our analysis ignores corrections for interstellar and/or circumstellar extinction.

The periods used in our analyses are those listed in the GCVS. Some uncertainty in the application of this period-luminosity relation results from the fact that Miras are not

TABLE 1

MIRAS WITH PERIODS BETWEEN 300 AND 400 DAYS AND $|b| > 30°$

Star	IRC	P(days)	f	l(°)	b(°)	m_K	D(pc)	|Z|(pc)	Δmag	Note
U Mic		334.29	39	0.92	-35.18	1.80	720	420	7.4	1
V Mic		381.15		1.33	-45.53	2.20	950	680	4.6	1
RT Sgr		306.46	47	2.06	-32.79	1.66	640	350	8.1	2
BD Oph		340.44		4.48	32.11	3.40	1500	810	4.6	2
WW Ser	+00268	365.8		8.65	44.98	1.75v	750	530	≥4.4	
S Ser	+10290	371.84	43	20.50	52.79	1.53v	690	550	7.1	
RV PsA		361		21.30	-47.40	6.55	6800	5000	≥2.5	2
RU Cap	-20590	347.37	36	22.94	-31.45	2.84v	1200	630	6.0	
R Ser	+20285	356.41	41	26.23	46.76	-0.01v	330	240	9.2	
UV Her	+10310	341.95		29.80	33.37	1.78v	730	400	5.5	
R Her		318.14	39	32.51	44.53	3.08	1300	880	6.8	1
S Her	+20307	307.28	47	33.61	33.10	1.49v	590	320	7.4	
RX Boo	+30257	340		34.28	69.21	-1.85v	140	130	2.7	
VY Her		300.38		37.69	30.52	3.51v	1500	750	≥4.9	2
BG Her	+20314	347.74		39.54	30.59	2.69v	1100	570	≥2.9	
VV Her	+30284	385.64	2	41.92	45.07	2.40v	1050	750	5.2	
TX Aqr		346.9		48.60	-30.39	5.34	3800	1900	≥4.0	2
S CrB	+30272	360.26	35	49.47	57.17	-0.20v	300	260	8.3	
KQ Her		345		50.87	31.63	4.29v	2300	1200	≥2.5	2
DU Aqr		372		54.82	-38.00				4.2	
UX Aqr		319.9		55.34	-64.36	3.43	1500	1300	≥4.9	3
RS CrB	+40276	332.2	47	57.61	49.57	1.77	710	540	2.9	
VY Peg		377.0		62.12	-39.77	3.48	1700	1100	≥5.0	2
EM Peg	+10500	356		63.23	-31.52	2.12	880	460	2.6	
V Peg	+10505	302.35	44	65.42	-37.07	3.05v	1200	720	8.0	
R Aqr	-20642	386.96	42	66.52	-70.32	-1.22v	200	190	6.5	
WW Her		312.37	40	72.12	33.86	4.86	2800	1600	5.6	2
T Peg	+10511	379.4	49	72.80	-34.07	2.15v	930	520	7.0	
AO Her		370		77.39	32.39	3.95	2100	1100	≥5.0	2
SY Dra	+50267	391.38		81.60	32.82	2.48v	1100	600	≥3.5	
R CVn	+40248	328.53	46	82.66	72.77	0.75v	440	420	6.4	
R Peg	+10527	378.1	44	85.41	-44.56	0.33v	400	280	6.9	
S Peg	+10533	319.22	47	88.35	-47.76	1.59	640	470	6.9	
EX Peg		337.24	25	90.65	-30.21	3.21	1400	700	9.0	2
W Peg	+30509	345.5	46	98.57	-32.22	-0.36	270	150	5.4	
S Cet	-10007	320.45	47	101.69	-71.06	3.36v	1400	1400	7.1	
AN Dra		353.5		103.33	33.95	3.39v	1600	870	4.2	2
R UMi	+70135	325.7	50	105.01	36.24	0.20v	340	200	3.0	
Z Peg	+30522	334.8	50	108.71	-35.56	1.35v	590	340	6.3	
U UMi	+70124	330.92	50	110.44	48.20	0.84v	460	340	5.9	
RV UMi		304		113.68	42.92	4.12	2000	1300	4.5	2
S UMi	+80030	331.0	50	114.05	35.61	0.26	350	210	≥5.7	
TU And	+30012	316.77	48	117.60	-36.65	2.05v	780	470	5.3	
T UMi	+70119	301.0	45	118.71	43.34	2.58v	960	660	7.2	
U CVn	+40238	345.65		127.06	78.72	2.84	1200	1200	≥3.7	
X Psc		349.6		129.22	-40.44	2.68	1100	730	≥5.2	1
TZ Psc		376.0		131.83	-36.95	4.02	2200	1300	≥4.8	2
Y Dra		325.79	45	133.80	34.95	2.64v	1050	600	8.8	2
R UMa	+70099	301.62	39	138.36	44.36	1.71v	650	450	7.2	
R Psc	+00019	344.50	44	141.94	-58.54	1.92	780	670	7.8	
T Ari	+20049	316.6	49	158.66	-37.12	0.30	350	210	3.8	
RU Ari		353.5	4	161.47	-41.92	2.73	1200	770	≥3.8	2
U Ari	+10040	371.73	40	166.14	-36.10	1.59v	710	420	8.0	
o Cet	+00030	331.96	38	167.75	-57.98	-2.40	100	88	8.1	
RT Lyn	+40193	394.6		183.62	31.97	2.92v	1400	720	≥2.5	
X Lyn		320.8		186.76	33.62	4.00	1900	1070	6.5	2
R LMi	+30215	372.19	41	190.59	49.77	-0.62v	260	200	6.9	
SS Eri		314.4		195.01	-53.75	4.07	2000	1600	≥3.6	2
BD Eri	+00062	336		195.56	-30.20	1.98v	790	400	4.3	
RY Cet	-20031	374		198.59	-69.59	2.60	1100	1060	≥3.0	

TABLE 1—*Continued*

Star	IRC	P(days)	f	l(°)	b(°)	m_K	D(pc)	|Z|(pc)	Δmag	Note
W Cnc	+30208	393.22	40	201.88	40.67	1.55v	720	470	7.0	
SV Leo		307.0	37	203.66	52.56	3.86	1800	1400	4.2	2
RT Eri	-20043	370.8	46	205.27	-50.81	0.11v	360	280	4.4	
U Cnc		304.78	40	206.32	31.19	4.63	2500	1300	7.0	1
TW Eri	-20039	322.2		214.62	-58.33	2.62	1030	880	4.2	
U For		318.50		220.19	-51.33	4.63	2600	2010	≥5.2	2
W Eri	-30033	376.73	40	222.17	-45.34	1.89	820	580	7.0	
T Lep	-20066	368.13	47	222.67	-32.72	0.33v	390	210	6.9	
R Leo	+10215	309.95	43	223.72	44.16	-2.4	99	69	6.9	
W Leo	+10234	391.75	35	233.02	59.43	2.59	1200	1000	5.9	
TZ Leo	+20228	331.5		235.33	67.24	2.15v	850	780	3.0	
R Cae		390.95	41	241.32	-41.32	0.47	440	290	7.0	1
R Com	+20237	362.82	38	248.03	76.32	2.14	900	870	7.5	
U Scl		333.73	39	248.18	-84.67	3.72	1800	1700	6.9	1
U Hor		348.4		252.88	-49.73	2.02	820	630	≥7.3	1
RT Crt		342.7		261.66	46.25	3.58	1700	1200	3.2	2
RT Hor		335		269.66	-49.74	4.42v	2400	1800	≥4.0	2
U Dor		394.4		274.30	-35.16	1.06	580	330	6.5	1
RX Dor		335.4		279.04	-35.18	4.46	2500	1400	5.4	1
S Hor		335.8		282.99	-53.78	3.37	1500	1200	≥3.0	1
Y Eri		302.7		284.35	-57.23	2.04	750	630	2.8	2
T Vir	-10264	339.47	36	286.55	55.66	2.77v	1100	940	5.8	
X Men		380		292.01	-37.04	1.49v	690	410	≥3.6	2
R Crv	-20237	317.03	41	292.65	42.98	1.50v	610	410	7.7	
SU Crv		351.5	37	293.80	40.38	3.44	1600	1030	3.8	2
W Phe		333.95	42	294.77	-60.76	2.63	1060	930	6.3	1
RY Hyi		319		299.34	-41.62	3.20	1300	890	4.5	2
FI Hya		324.1		299.75	36.12	3.75	1700	1030	7.2	1
X Hyi		308.5		303.57	-37.08	2.38	890	540	3.2	2
RU Oct		373		303.76	-30.89	2.84	1300	650	4.8	2
R Hya	-20254	388.87	49	314.22	38.75	-2.5	110	69	7.4	1
V663 Cen		310		314.98	30.96	4.41	2300	1200	≥4.9	2
W Hya	-30207	361	50	318.02	32.81	-3.1	80	43	3.9	1
S Vir	-10290	375.10	45	320.77	54.23	0.57v	450	360	6.9	
FQ Hya		355		321.47	34.57	6.38	6200	3500	3.3	2
RU Hya	-30215	331.5	35	323.37	30.79	1.56	640	330	7.1	
UU Tuc		335		329.05	-47.99	2.60v	1050	780	3.2	2
Z Vir		305.71	39	330.75	45.26	4.6	2500	1800	5.2	1
SX Lib		332.9		335.50	35.52	3.64	1700	980	≥5.6	2
S Pav		380.86	49	338.05	-31.12	-1.04	210	110	3.8	2
Y Ind		304.18	52	343.32	-46.99	2.68	1020	740	≥3.2	2
S Ind		399.95	41	343.37	-39.76	1.24	630	410	9.1	1
X Tel		309.8		345.94	-34.28	4.39v	2300	1300	3.6	2
RU Lib	-20289	316.56	46	350.61	32.18	2.64	1030	550	7.2	
R Gru		331.96	42	351.44	-49.24	1.66	680	510	7.5	1
RS Vir	+00243	353.95	37	352.67	57.97	1.48v	650	550	7.6	
S Scl	-30006	362.57	48	358.67	-80.75	0.39v	400	390	8.1	

[1] m_K from Gezari et al. 1987.
[2] m_K extrapolated from the *IRAS* Point Source Catalog 12 μm flux and eq. (3).
[3] Star No. 19 in Table 2 of Bothun et al. 1991.

strictly periodic. For example, R Aql has decreased from 320 to 284 days over a 60 yr interval (see the review by Wood 1990). We assume that stars with large variations in their periods are relatively rare, since previous kinematic studies (Feast 1963), and the results presented here show that different period Miras are in fact distinct populations.

Many of the K-band measurements used in our analysis come from the Two Micron Sky Survey (Neugebauer & Leighton 1969). For Miras that are too faint or too far south for that survey, other resources were used to obtain K band magnitudes. In some cases, K band data were listed in the compilation of infrared observations by Gezari, Schmitz, & Mead (1987) which includes the extensive set of K-band measurements of Miras by Catchpole et al. (1979).

TABLE 2

MIRAS WITH PERIODS LESS THAN 300 DAYS AND $|b| > 30°$

Star	IRC	P(days)	f	l(°)	b(°)	m_K	D(pc)	|Z|(pc)	Δmag	Note
RY Mic		198.2		1.83	-40.69	5.49	2800	1800	≥4.9	1
T Gru		136.49	48	4.78	-57.73	5.24	1900	1600	4.5	2
BG Ser	+00269	143		5.13	39.53	0.36	210	130	4.0	
BE Oph		231.5		6.25	30.31				≥4.0	
RY PsA		224.39		7.99	-50.21	4.93	2300	1800	≥5.2	1
TT Scl		133.3		8.62	-81.82	7.96	6500	6500	2.7	2
ST PsA		179		9.55	-63.92	5.99	3200	2900	≥3.5	1
AI Ser		212.5		10.93	35.61	5.88	3500	2000	4.5	1
DW Ser		235		11.12	37.04	5.73	3500	2100	3.5	1
X Mic		239.64		11.17	-41.19	3.73	1400	920	≥4.5	1
CM Ser		221.6		12.09	32.50	5.23	2600	1400	4.2	1
BC Ser		245.0		12.45	38.28	4.75	2300	1400	≥4.0	1
RS Mic		228.5		14.97	-32.74	5.22	2700	1500	5.5	1
R Mic		138.62	46	15.41	-35.14	3.89	1030	590	5.5	1
S Mic		209.68	43	16.83	-45.31	4.71	2000	1400	7.0	2
RX Mic		239.75		17.65	-37.96	4.81	2300	1400	≥4.5	1
RR Cap		277.54	40	19.00	-39.49	3.45	1400	870	7.7	2
R PsA		297.6	38	19.51	-56.31	3.21	1300	1060	6.4	2
U Boo		201.31	50	20.99	60.17	5.38	2600	2300	3.2	2
S PsA		271.7	42	21.51	-53.02	3.62	1500	1200	6.5	2
U Ser		237.50	48	22.16	40.86	3.61	1300	860	6.9	2
SS Her		107.36	48	22.46	33.82	5.19	1600	870	5.0	2
V Cap		275.72	42	23.38	-39.82	2.99v	1100	700	6.2	1
X Cap		217.94	48	26.64	-39.26	6.37	4400	2800	4.8	1
TX Cap		129.35		28.80	-31.58	6.21	2900	1500	≥3.6	1
V440 Oph		276.9		31.67	30.36	4.35	2100	1000	≥5.0	1
AS Her	+10309	269.14	53	31.14	35.65	2.15v	730	430	5.4	
U Cap		203.14	46	32.11	-32.40	6.42	4300	2300	5.3	3
Z Cap		181.48	49	33.08	-37.94	5.20	2300	1400	6.4	2
RT Aqr	-20618	246.3		33.25	-56.05	2.18v	700	580	4.3	
AQ Aqr		235.6		33.52	-53.49	6.27	4400	3600	≥3.5	1
AH Ser		283.5		33.65	46.54	4.57	2300	1700	3.7	1
V361 Her		85		35.36	41.15				3.0	
T Cap		269.28	44	35.63	-40.08	3.28	1200	790	5.9	2
BF Her		196		37.15	30.98	4.85	2000	1050	2.5	1
AV Aqr		251.3		37.23	-55.59	6.71	5700	4700	≥4.5	3
R Boo	+30260	223.40	46	38.07	66.47	1.99v	600	550	6.9	
S Aqr	-20624	279.27	39	41.31	-63.04	2.80v	1000	900	7.4	
DO Her		216.28	50	41.51	40.69	6.50	4700	3000	5.6	1
SY Her		116.91	49	43.02	33.64	4.24	1100	600	5.6	2
MV Her		222		43.10	34.47	3.71	1300	740	≥3.0	1
SS Aqr		192.6	55	45.01	-52.54	4.71	1900	1500	4.6	2
RS Aqr		214.62	49	46.51	-32.67	4.79	2100	1100	4.9	2
Z CrB		250.68	42	47.12	49.51	4.19	1800	1400	6.7	2
RR Aqr		182.45	44	48.28	-32.97	5.60	2700	1500	5.3	2
RT Her		298.08	40	49.01	32.99	3.07v	1200	650	7.0	1
KR Her		135.9		51.13	31.62	4.60	1400	740	≥3.1	1
HU Her		166	45	51.50	42.72				2.9	
RV Her		205.23	44	53.23	36.19	5.42	2700	1600	6.5	1
RW Aqr		139.57	38	53.32	-32.69	5.43	2100	1100	4.9	1
HT Her		163.15	48	55.65	43.21				4.4	
WW Aqr		241.18		57.16	-34.06	6.05	4100	2300	4.0	1
TY Aqr		213		57.20	-38.10	6.71	5100	3100	≥4.2	1
X CrB		241.17	46	57.96	51.51	3.66	1400	1060	5.7	2
WX Her		186		58.55	31.64				4.3	

TABLE 2—*Continued*

Star	IRC	P(days)	f	l(°)	b(°)	m_K	d(pc)	|Z|(pc)	Δmag	Note
RT Boo	+40265	273.86	49	58.82	57.87	2.56v	890	760	5.6	
W Her	+40285	280.03	45	60.02	42.29	2.90v	1060	710	6.8	
W CrB		238.40	45	60.36	46.23	3.69	1400	990	6.5	1
WY Aqr		245.2		64.05	-42.66	5.64	3400	2300	≥4.0	1
RT CVn		253.60	45	64.41	76.04	5.25	2900	2800	4.0	1
RR Boo		194.70	48	67.23	63.08	5.03v	2200	2000	5.6	1
V Boo	+40257	258.01	49	68.96	66.39	0.93v	410	370	5.0	
Z Aqr		135.5	33	69.30	-72.23	3.63	900	860	2.5	2
DM Aqr		157		70.79	-60.45				≥3.7	
DG Peg		146.60		72.94	-32.11				4.1	
Y Peg		206.93	46	74.90	-33.22	5.69	3100	1700	7.1	2
V Cet		257.82	45	85.58	-67.86	4.05	1700	1600	6.2	2
RW Peg		208.43	48	88.19	-40.23	4.84	2100	1400	5.8	2
FF Peg		252.4		94.08	-48.79	4.56	2100	1600	5.0	1
S Boo		270.73	44	96.93	58.46	3.22	1200	1030	6.0	1
R Dra	+70136	245.60	45	98.53	38.24	2.16v	690	430	6.5	
RR Psc		270.6		101.15	-54.27	6.14	4600	3700	≥3.9	1
DL Peg		180.4		101.39	-44.56	6.19	3600	2500	≥5.3	1
DU Peg	+30520	161.3		107.76	-31.34	2.78v	690	360	≥4.0	
UW And		244.2		113.21	-33.12	4.92	2400	1300	≥4.6	1
T And	+30009	280.76	46	114.98	-35.43	3.16v	1200	700	6.8	
T Psc	+10005	252		115.90	-48.01	2.15	700	520	3.3	
RR UMa		230.58	43	116.09	54.29	5.04	2500	2000	5.6	1
YZ And		207.65		116.83	-31.69	4.56	1900	970	≥4.5	1
W Psc		188.1	48	125.18	-34.89	5.88	3200	1800	3.4	1
RV Dra		208.14	35	125.23	51.50	5.76	3200	2500	5.8	1
RS UMa		258.97	42	126.06	58.57	3.56v	1400	1200	6.6	1
T UMa	+60219	256.60	41	126.49	57.54	2.78v	950	800	6.9	
Z Cet		184.81	48	131.72	-64.09	3.21	920	830	5.8	2
RX Psc		280.54	43	133.47	-40.77	5.76	4000	2600	5.8	1
VX UMa	+70102	215.2		134.72	42.51	2.70v	810	550	≥2.8	
U Psc		173.1	48	134.76	-49.28	6.51	4000	3000	4.6	2
Z UMa	+60213	195.5		136.63	57.77	0.89v	330	280	3.2	
SW Cam		252.8		141.39	31.05	5.88	3900	2000	3.5	1
Z Tri		216.1		142.86	-31.96	5.40	2800	1500	3.6	1
R Ari		186.78	45	146.16	-33.97	3.96	1300	730	6.3	2
S Ari		292.15	45	149.39	-46.55	4.76	2600	1900	6.0	2
RT Ari		262.81		161.34	-33.17	4.65	2300	1200	5.5	1
R Cet	+00032	166.24	43	166.97	-54.75	3.04v	790	640	6.8	
T CVn	+30239	290.09	42	168.26	83.63	2.05v	740	730	5.0	
X UMa		249.04	43	168.98	37.74	4.81v	2400	1400	6.7	1
RU UMa		252.46	30	170.68	71.52	4.07	1700	1600	6.9	1
W Lyn		295.2		180.83	32.78	4.12v	1900	1050	6.5	1
X Cet		177.14	49	182.92	-45.98	4.21	1400	1000	4.6	2
U Cet	-10035	234.76	44	187.70	-62.31	2.95v	960	850	6.6	
U LMi	+40213	272.2	40	188.15	51.65	2.87	1030	810	3.3	
S LMi		233.83	42	190.02	51.46	3.83	1400	1100	6.8	1
W LMi		117.2	46	207.84	61.71				3.0	
V Leo		273.35	44	211.92	50.66	3.28	1200	960	6.0	2
RS Leo		208.2	31	212.11	46.53	4.30	1600	1200	5.3	1
RS Eri	-20052	296.00		214.02	-41.97	1.43v	560	380	≥3.6	
T Eri	-20047	252.29	45	219.27	-48.66	2.57v	850	640	6.0	
U Eri		274.91	49	220.25	-49.93	4.43	2100	1600	6.4	1
AO Leo		150		221.40	72.25				2.5	
RY Leo		155	47	223.00	48.94	5.22	2100	1500	2.8	1

TABLE 2—*Continued*

Star	IRC	P(days)	f	l(°)	b(°)	m_K	d(pc)	|Z|(pc)	Δmag	Note
AB Com		194.7		236.49	81.85				≥2.6	
T Col		225.84	50	237.22	-32.87	1.90	580	310	6.1	2
S Sex		264.9	50	247.24	47.22	3.52	1400	1000	5.5	2
S Leo		190.16	47	250.57	57.71	6.07	3500	3000	5.5	1
TX Hor		287.37	45	252.34	-47.75	4.54	2300	1700	2.8	1
T Pic		200.58	49	252.91	-35.53	4.22	1500	900	6.5	2
R Pic		170.9		255.90	-40.35	3.34	920	600	3.7	2
RY Pic		219		263.63	-32.41	2.90	900	480	≥3.5	1
SU Dor		235.86		264.21	-39.41	5.16	2700	1700	≥5.5	1
SU Vir		208.6	48	264.44	71.69	5.05	2300	2200	6.1	2
U Crt		169	45	264.63	48.10	5.96	3100	2300	≥4.0	1
T Hor		217.60	48	265.53	-56.03	3.34	1100	910	6.5	2
T Dor		168.0		269.46	-38.86	3.38	930	580	≥3.5	2
R Ret		278.46	48	273.99	-39.41	1.83	650	410	7.7	2
RV Ret		269.5		276.22	-44.39	4.46	2100	1500	5.1	1
Y Crt		158.36	50	278.06	33.52	5.06	1900	1100	≥4.8	1
RT Men		250.44	44	282.50	-36.55	6.37	4900	2900	5.0	1
SV Vir	-10260	295.33		282.85	50.68	3.12v	1200	940	≥3.2	
DO Com		130		283.24	80.90				2.8	
ST Crv		224.6		284.06	47.72	4.62	2000	1500	≥3.3	1
RS Hor		202.85		284.32	-50.61	4.66	1900	1500	≥5.2	1
R Men		120?		286.53	-30.52	2.08	400	210	2.5	2
IR Hya		187.7	35	288.09	35.68				4.5	
WY Hyi		231		288.62	-37.71	6.68	5300	3200	≥3.6	1
R Vir	+10256	145.63	50	293.68	69.63	2.24v	500	470	6.0	
Y Vir		218.43	46	294.61	58.17	4.72	2100	1800	6.7	2
BL Hya		146		296.45	31.19				4.0	
RS Phe		239		296.74	-60.12				≥3.9	
U Crv		283.42		297.50	44.24	4.15	1900	1300	≥4.9	1
V Crv		193.63		299.25	45.15	7.07	5600	4000	≥3.8	3
EO Hya		291.97		300.36	36.95	4.97	2800	1700	≥3.8	1
RS Hyi		215.5		301.53	-40.24	5.06v	2400	1500	6.0	1
U Tuc		264.8	46	302.43	-42.12	2.79	970	650	6.8	2
U Vir		206.64	47	302.70	68.42	4.08	1500	1400	6.1	2
V473 Cen		224		302.73	31.65	6.50	4800	2500	≥3.6	3
TZ Tuc		239.92		302.74	-47.24	4.37	1900	1400	≥5.5	1
CM Hya	-30196	295		302.78	33.02	2.51	920	500	3.0	
EP Hya		166.00		303.01	36.09	4.17	1300	780	≥4.7	1
W Hyi		281		304.00	-37.41	5.86v	4200	2500	3.1	1
V487 Cen		260		304.65	31.26				3.7	
X Scl		261.63	50	305.86	-82.20	3.91	1600	1600	4.6	2
SW Hya		218.8		306.06	33.70	3.55	1200	670	≥3.2	1
BZ Vir		150.92		306.07	45.17	4.85	1700	1200	≥3.5	1
S Tuc		240.71	44	308.80	-55.13	4.30v	1800	1500	6.8	1
RV Vir		265.87	41	309.12	49.51	5.19	2900	2200	4.9	2
U Phe		226.3		309.57	-66.71				≥4.4	
T Oct		218.50	51	310.46	-31.53	3.42	1100	590	6.0	1
RX Com		211.11		311.68	77.94				≥4.5	
R Tuc		286.06	41	311.78	-50.81	3.01v	1100	880	6.7	1
T Phe		281.79	37	313.72	-70.27	3.26	1300	1200	5.9	2
VY Vir		280.04		315.57	57.52	3.37	1300	1100	4.2	1
SX Vir		105.55		317.28	42.02	3.48	710	470	3.1	1
RR Oct		272.83		318.47	-34.02	3.82v	1600	890	≥3.4	1
Z Phe		255		319.64	-61.99	4.70	2300	2000	≥5.0	1
V Vir		250.08	42	320.48	58.46	4.08	1700	1400	6.9	1

TABLE 2—*Continued*

Star	IRC	P(days)	f	l(°)	b(°)	m_K	D(pc)	|Z|(pc)	Δmag	Note
R Ind		216.26	47	320.61	-44.91	4.22	1600	1200	6.4	2
RW Ind		150		321.73	-41.03	6.01	2900	1900	≥3.8	1
SS Ind		190	47	323.25	-42.98	5.48	2700	1800	5.2	1
T Pav		243.62	43	323.43	-30.29	2.99	1010	510	7.0	1
R Phe		269.26	50	324.22	-65.01	3.15	1200	1050	6.9	2
SV Pav		210		324.65	-33.76	6.39	4300	2400	≥2.7	1
T Scl		202.42	49	324.97	-78.25	3.95	1400	1300	5.0	1
BQ Pav		112	54	325.53	-31.25	7.03	3800	2000	≥3.1	3
T Tuc		250.3	46	326.16	-49.25	2.96	1010	770	6.3	2
AA Tuc		216.9		329.64	-48.18	5.63	3100	2300	≥3.0	1
RR Vir		217.52	47	331.57	49.55				4.9	
SY Vir		236.65	57	332.58	54.38	4.73	2200	1800	3.8	1
U Pav		289.7		332.84	-37.99	3.12	1200	740	≥3.4	1
RR Pav		239.8		333.05	-32.42	4.75	2200	1200	≥3.0	1
EP Lib		185.78	46	333.38	33.80	5.53	2700	1500	≥3.2	1
TW Lib		135.5		336.38	35.86	5.96	2600	1500	5.4	1
V Lib		255.30	42	336.53	38.01	4.69	2300	1400	6.9	2
V Scl		296.1	48	336.62	-74.97	3.08	1200	1200	6.3	1
SU Pav		245.3		336.95	-33.94	4.06	1700	920	≥5.6	1
SV Phe		265		337.20	-69.64	4.66	2300	2200	4.8	3
V Phe		257.00	47	337.41	-65.50	3.17	1100	1030	5.9	2
CF Vir		227.6		337.76	51.22	5.03	2500	1900	≥3.0	1
BR Pav		246.13	50	340.27	-32.95	4.13v	1700	930	5.5	1
RY Pav		236.3		340.83	-31.87	5.55	3200	1700	≥4.0	1
YY Lib		229.53		340.84	31.46	4.53	2000	1020	≥3.0	1
BQ Tel		290		341.60	-34.59	3.32v	1300	750	6.3	1
BP Tel		241		342.10	-33.02	4.73	2200	1200	6.2	1
RT Lib		251.16	45	342.15	33.66	4.40	2000	1090	6.5	2
T Lib		237.50	41	342.20	32.03	5.89	3800	2000	5.4	1
X Ind		222.85	49	342.46	-44.72	3.43	1200	810	≥4.0	1
S Lib		192.9	49	344.24	30.20	4.55	1800	880	5.5	2
TT Lib		278.3		345.11	35.87	4.14	1900	1100	5.1	1
AQ Vir		292.8		346.08	45.73	4.11	1900	1400	4.8	1,4
XY Vir		258.1		346.09	47.56				≥2.8	
RZ Ind		255		349.51	-41.49	3.33	1200	800	≥5.6	1
AO Vir		254.61	43	349.80	58.30	4.03	1700	1400	2.5	1
W Lib		205.50	45	350.87	30.82	7.28	6400	3300	5.0	3
Y Lib		275.7	41	353.83	42.59	3.16	1200	800	7.1	2
CL Lib		150		354.24	33.85				≥3.0	
TZ Lib		183.6		355.78	35.31	5.68	2900	1600	4.7	1
XY Mic		150		356.04	-40.78				3.0	
SW Lib	-10327	291.8		357.10	30.07	2.66	980	490	5.3	
AL Boo		168		357.55	76.18				2.9	
EE Lib		208.9		357.81	34.57	3.49	1100	650	≥3.3	1
Z Boo		281.14	39	358.76	67.79	3.77	1600	1500	6.8	2
W Mic		198.8		359.53	-45.34	5.65	3000	2100	5.2	2

NOTE.—The variable sources in the TMSS or in the *IRAS* catalog have mK designated by v; at some level, all the sources are variable.

[1] m_K extrapolated from the *IRAS* Point Source Catalog 12 μm flux and eq. (4).

[2] m_K from Gezari et al. 1987.

[3] m_K extrapolated from the *IRAS* Faint Source Catalog 12 μm flux and eq. (4).

[4] Three are minutes offset between *IRAS* position and that given by Kholopov et al. 1985.

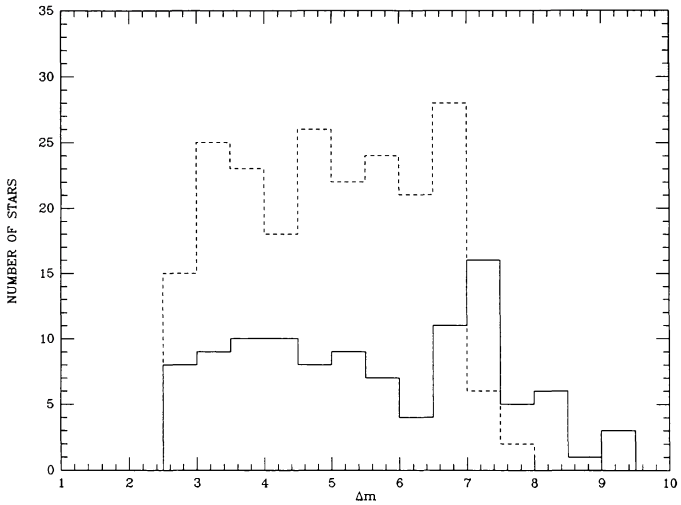

FIG. 1.—Histogram of the amplitude variations of the Miras listed in Tables 1 and 2 as reported by Kholopov et al. (1985). The dashed line refers to Miras with $P < 300$ days while the solid line refers to Miras with 300 days $< P < 400$ days.

The K-band photometry is usually reasonably consistent between different sets of measurements. We display in Figure 2 a histogram of the difference of the K magnitudes from the TMSS and those from the survey of Miras by Catchpole et al. (1979) for the 34 stars that they have in common in our biconical search zone. Most stars display a relatively small variation of less than 0.5 mag between the two surveys. However, two stars, R Ser and R Aqr exhibit large deviations between the two surveys. In particular, R Aqr is noteworthy because the three K-band measurements in the TMSS (obtained during the 1960s) range from −1.09 to −1.55 mag, while the 17 measurements in the survey by Catchpole et al. (1979) obtained during the 1970s range from −0.10 to 0.88 mag. During the early 1980s the K magnitude of R Aqr returned to near −1 mag (Kenyon & Gallagher 1983; Whitelock et al. 1983).

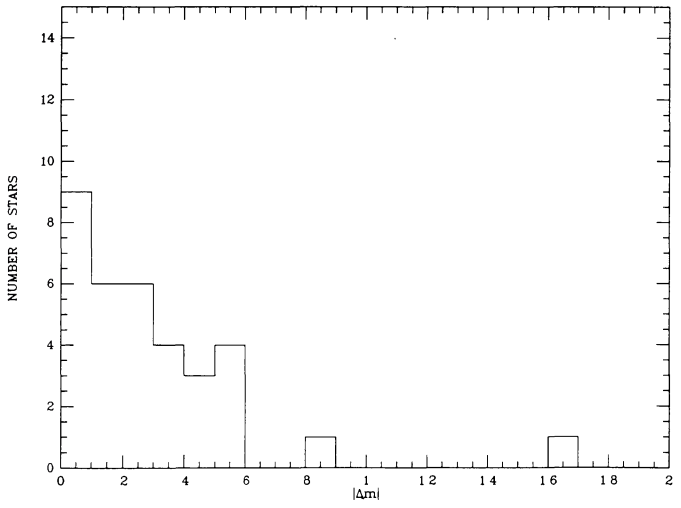

FIG. 2.—Histogram of the value of $|m_K(\text{TMSS}) - m_K(\text{SAAO})|$ which compares the data from the TMSS (Neugebauer & Leighton 1969) with that from the South African Astronomical Observatory (Catchpole et al. 1979). We compute m_K(SAAO) from the midpoint of the minimum and maximum measured for this quantity in the data set given by Catchpole et al. (1979). The point near 0.9 mag is R Ser while the point near 1.4 mag is R Aqr which is discussed in the text.

If we are unable to find K-band photometry, we estimate m_K from the flux measured by *IRAS* at 12 μm because there is a relatively small dispersion of $F_\nu(2.2\ \mu\text{m})/F_\nu(12\ \mu\text{m})$. Specifically, for the 162 Miras in both the Two Micron Sky Survey and *IRAS* data base with periods in the range 300 days $< P <$ 400 days, we show a histogram of $F_\nu(12\ \mu\text{m})/F_\nu(2.2\ \mu\text{m})$ in Figure 3. We take the non–color corrected flux at 12 μm from either the *IRAS* Point Source Catalog or the *IRAS* Faint Source Catalog (1991; magnetic tape version) and we take the 2 μm magnitude from the Two Micron Sky Survey using the calibration that 0.0 mag corresponds to 620 Jy from Beckwith et al. (1976). We find that the median flux ratio is

$$F_\nu(12\ \mu\text{m})/F_\nu(2.2\ \mu\text{m}) = 0.31\ . \qquad (3)$$

About 67% of these intermediate-period Miras obey equation (3) to better than a factor of 1.5.

Similarly, for the 81 Miras with periods less than 300 days that were observed both by the TMSS and by *IRAS*, we show a histogram of the observed ratio for this quantity in Figure 3. The median of the flux ratio in the sample is

$$F_\nu(12\ \mu\text{m})/F_\nu(2.2\ \mu\text{m}) = 0.25\ . \qquad (4)$$

We find that equation (4) is accurate to within a factor of 1.5 for over 80% of these short-period Miras. This factor of 1.5 in the flux translates into a factor of $(1.5)^{1/2}$ or about a factor of 1.2 random uncertainty in the distance estimate. For 21 of the stars in Table 2, we are unable to find infrared photometry; we do not estimate distances to these stars.

Most of the stars in Tables 1 and 2 that were also found in the TMSS are known to be variable at 2.2 μm and are noted as such in these tables. In most cases, the range of the variation at K is less than 1.0 mag.

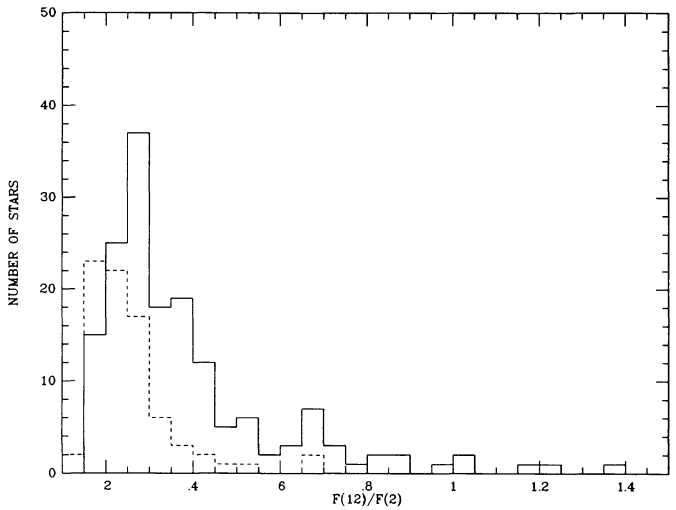

FIG. 3.—Histogram of the flux ratio $F_\nu(12\ \mu\text{m})/F_\nu(2.2\ \mu\text{m})$ for all the Miras in the Two Micron Sky Survey. The dashed line refers Miras with $P < 300$ days, while the solid line refers to Miras with 300 days $< P < 400$ days.

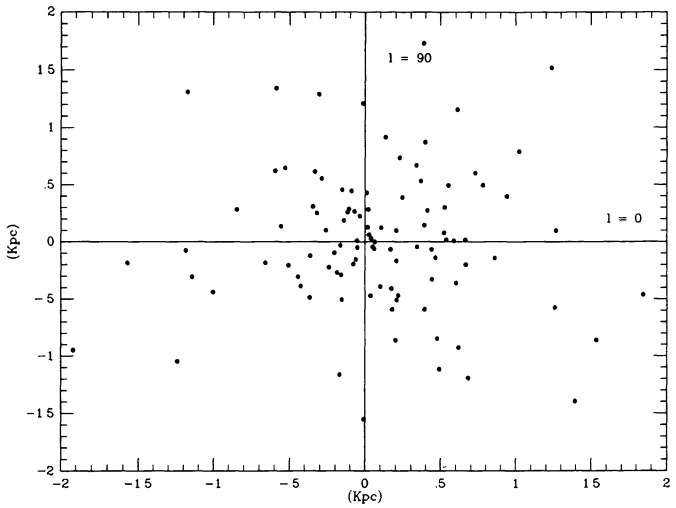

FIG. 4.—The projection onto the Galactic plane of the intermediate-period Miras listed in Table 1.

For a few of the intermediate-period Miras stars not listed in the TMSS but lying in the relevant declination zone, Y Dra, RU Ari, and X Psc, we estimate K magnitudes somewhat brighter than the limit of 3.0 mag for the Two Micron Sky Survey. In fact, Catchpole et al. (1979) report 10 observations of X Psc, all of which are brighter than $m_K = 3.0$ mag and the midpoint between their maximum and minimum of their measured K brightness is 2.75 mag, quite close to our predicted value of $m_K = 2.68$ mag. It is possible that X Psc has undergone some systematic drift in its brightness during the past few decades. For one intermediate-period Mira in Table 1, DU Aqr, we have been unable to find infrared photometry of any sort; we do not estimate its distance.

3. INTERMEDIATE-PERIOD MIRAS

3.1. *Space Distribution*

We consider the 107 Miras listed in Table 1 with periods in the interval 300–400 days and approximate their spatial density, n, with a function of the form:

$$n = n_0 \exp(-|Z|/Z_0) \exp[-(R - R_*)/R_0] . \quad (5)$$

In equation (5), Z is the distance from the Galactic plane, Z_0 is the exponential scale height, R is the Galactocentric radius of the star, R_* is the Galactocentric radius of the Sun, and R_0 is the scale length in the Galactic disk.

Figure 4 shows a projection onto the plane of the Milky Way of the spatial locations of intermediate-period Miras from Table 1. We find that there is a modest excess of stars in the hemisphere facing the Galactic center (61 Miras) compared to the hemisphere facing the anticenter (44 Miras). We estimate the scale length in the Galactic plane, R_0, by comparing the longitude zone 330°–30° (20 stars) with the longitude zone 150°–210° (14 stars). The median distances projected onto the Galactic plane of both sets of stars is 700 pc. Since the surface density of the sample of stars at high latitudes in our search zone varies by a factor of 1.5 over a change in Galactocentric radius of 1400 pc, we deduce $R_0 \sim 3500$ pc. This result is slightly smaller than the value of 4500 pc derived by Habing (1988) for the "thin disk" red *IRAS* sources.

With such a large estimated value for R_0, we can ignore the variation of density, n, with R in estimating the scale height of intermediate-period Miras from equation (5). With this approximation, equation (5) predicts that the number of stars within our biconical search zone is

$$N_* = 4\pi n_0 Z_0^3 \cot^2 b_{cr} , \quad (6)$$

where b_{cr} is the absolute value of the minimum Galactic latitude of our sample. Equation (6) implies that the scale height can be estimated directly from the median height above the Galactic plane:

$$Z_{med} = 2.7 Z_0 . \quad (7)$$

We find that for the 107 stars in Table 1, $Z_{med} = 650$ pc. In the hemisphere facing the anticenter, the median height is 700 pc, while for the hemisphere facing the Galactic center, the median height is 600 pc; there does not appear to be any significant difference in the two directions. From the median height of the entire sample of 650 pc we deduce an exponential scale height for the intermediate-period Miras of 240 pc.

We show in Figure 5 a comparison of the theoretical model given by equation (5) with the observed distribution of stars vertical to the plane. We also compare models with scale heights that are a factor of 1.5 larger and 1.5 smaller than our estimated value of 240 pc. The model with $Z_0 = 240$ pc agrees much better with the data. This value for the exponential scale height agrees with the value of between 200 and 250 pc derived by Habing (1988) for the "thin disk" red *IRAS* sources and is close to the value of ~200 pc derived by Jura & Kleinmann (1989) for the "very dusty" AGB stars in the Solar neighborhood.

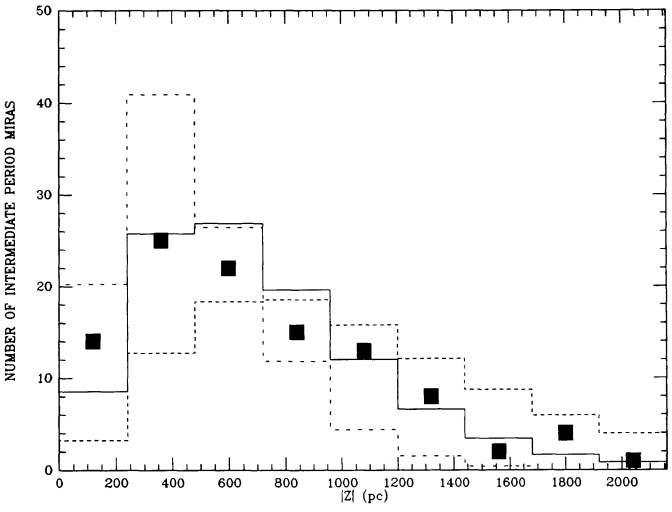

FIG. 5.—A histogram of the distribution of distances from the Galactic plane of the intermediate-period Miras listed in Table 1, compared with the exponential distribution given by eq. (5). The solid curve is for Z_0 = 240 pc, our inferred value of the exponential scale height, while the dashed curve is for Z_0 = 360 pc, and the dot-dashed curve is for Z_0 = 160 pc.

From the inferred exponential scale height of 240 pc, and since $N_* = 107$, we find from equation (6) that $n_0 = 210$ kpc^{-3}. The projected surface density, σ, of these stars onto the Galactic plane is

$$\sigma = 2n_0 Z_0 , \quad (8)$$

Consequently, we find for the Miras in the period range between 300 and 400 days that $\sigma = 100$ kpc^{-2}. This result for the surface density of the oxygen-rich Miras is a factor of 3 larger than the value of 33 kpc^{-2} derived by Habing (1988) for the "thin disk" red *IRAS* sources and a factor of 4 larger than the value of 25 kpc^{-2} derived by Jura & Kleinmann (1989) for the "very dusty" stars in the solar neighborhood.

Our observationally derived exponential scale height of ~240 pc for the intermediate-period Miras is equal to that of main-sequence stars of slightly more than 1 $M_\odot$ (Miller & Scalo 1979). Therefore, we infer that such stars are the progenitors of intermediate-period Miras. Theoretical analysis of the pulsation periods (see, for example, Wyatt & Cahn 1983, Wood 1990), also suggests that Miras with periods in the range $300 < P < 400$ days have main-sequence progenitors in this mass range. Stars with masses of ~1.4 $M_\odot$ or greater have exponential scale heights of 150 pc or less (Miller & Scalo 1979) and therefore most of them probably do not become intermediate-period Miras.

Miller & Scalo (1979) have found that the space density for the main-sequence stars in the mass range 1.0–1.2 $M_\odot$ equals 5.1 10^6 kpc^{-3}. From their calculated lifetimes, Miller & Scalo estimate that the death rate, dn_{ms}/dt of these stars is 8.6×10^{-4} kpc^{-3} yr^{-1}. We write for the lifetime of the Mira phase, t_{Mi} that

$$t_{Mi} = n_0/(dn_{ms}/dt) . \quad (9)$$

Since we estimate n_0 is ~210 kpc^{-3}, this implies that t_{Mi} is $\sim 2 \times 10^5$ yr.

Wood (1990) derived a shorter lifetime for the Mira phase —5×10^4 yr—by assuming that all planetary nebulae evolve from oxygen-rich Miras. He estimated the total numbers of both Miras and planetary nebulae in the Galaxy, N_{Mi}, by extrapolating from the densities given by Cahn & Wyatt (1976) and Wood & Cahn (1977) who, however, did not separate the Miras according to period. (Since, however, the total space density of Miras is dominated by the intermediate-period objects [see Table 4], this is not a major effect.) Adopting a lifetime for planetaries, t_{PN}, of 2×10^4 yr, he obtained

$$t_{Mi} = (N_{Mi}/N_{PN})t_{PN} . \quad (10)$$

We disagree with Wood's result because we have distinguished the Miras by their different populations. As noted by Zuckerman & Aller (1986), about half of all local planetaries are carbon-rich as are about half of all the apparent preplanetary red giant stars that are losing mass at a rate in excess of 2×10^{-6} $M_\odot$ yr^{-1} (Jura & Kleinmann 1989). Including carbon-rich planetaries in N_{PN} may therefore lead to a low estimate of t_{Mi} for the oxygen-rich Miras.

3.2. *Mass-Loss Rates*

Although it is clear that Miras lose substantial amounts of mass, there are some significant uncertainties in estimating the mass-loss rates (van der Veen & Rugers 1989). Here, we note that there is reasonably good agreement between recent mass-loss rates inferred from observations of circumstellar CO emission and mass loss rates plausibly inferred from *IRAS* measurements of the far-infrared flux. Bujarrabal, Gómez-González, & Palnesas (1989) have measured CO radio emission from five of the nearest intermediate-period Miras listed in Table 1. From their data, they can determine terminal velocities of the gas, v_∞, and mass-loss rates, dM/dt. We report their results in Table 3 after scaling dM/dt by D^2 to the distances, D, that we use in Table 1 rather than use the distances used by Bujarrabal et al. (1989).

From analysis of both oxygen-rich and carbon-rich stars, Jura (1987) proposed that the mass-loss rate, dM/dt ($M_\odot$ yr^{-1}), may be estimated by the formula:

$$dM/dt = 1.1 \times 10^{-8} v_{dust} D_{kpc}^2 L_4^{-1/2} F_\nu(60) \lambda_{10}^{1/2} , \quad (11)$$

where v_{dust} is measured in km s^{-1}, L_4 is the luminosity ($10^4 L_\odot$), $F_\nu(60)$ is the non–color-corrected flux at 60 μm measured by *IRAS* (Jy), and λ_{10} is the average wavelength of the emitted light from the system (10 μm). The basic physics of this equation is discussed by Sopka et al. (1985). Implicit in the use of the value of the numerical coefficient in this equation are "standard" values for the dust to gas ratio and far-infrared emissivity of the dust grains. These parameters are not well known and may vary from star to star. Nevertheless, equation (11) seems to be useful for estimating mass-loss rates to within a factor of 2.

From Wood (1990), we take $L_4 = 0.5$, and for these oxygen-rich Miras, we adopt $\lambda_{10} = 0.15$. The distances are taken from Table 1 and $F_\nu(60)$ from the *IRAS* Point Source Catalog. In the outflows from red giants, the dust grains are driven supersonically through the gas by radiation pressure with streaming velocity, v_{st} (see, for example, Kwan & Linke 1982). If v_∞ is the gas outflow velocity, we may write that v_{dust} is the sum of these two velocities:

$$v_{dust} = v_\infty + v_{st} \quad (12)$$

In previous studies of mass-losing stars, we have assumed for simplicity that $v_{dust} = v_\infty$ (Jura 1987). This approximation is appropriate when the mass-loss rate is very large, and there is a large amount of frictional drag on the dust grains. However, for stars losing relatively small amounts of mass, the grain

TABLE 3

MASS-LOSS RATES FOR NEARBY INTERMEDIATE PERIOD MIRAS

Star	v_∞ (km s^{-1})	$F\nu(60)$ (Jy)	dM/dt_{gas}	dM/dt_{dust}
S CrB	5.5	19.0	3.1	1.1
R Leo	5.1	114	1.0	0.85
R LMi	6.4	26	2.8	1.5
RX Boo	8.6	69	1.9	1.6
W Hya	6.0	195	0.61	1.0

NOTES.—The mass-loss rates either are extrapolated from CO observations (dM/dt_{gas}) performed by Bujarrabal et al. 1989 or they are extrapolated from *IRAS* measurements (dM/dt_{dust}) by using eq. (11). The mass-loss rates are expressed in units of 10^{-7} $M_\odot$ yr^{-1}.

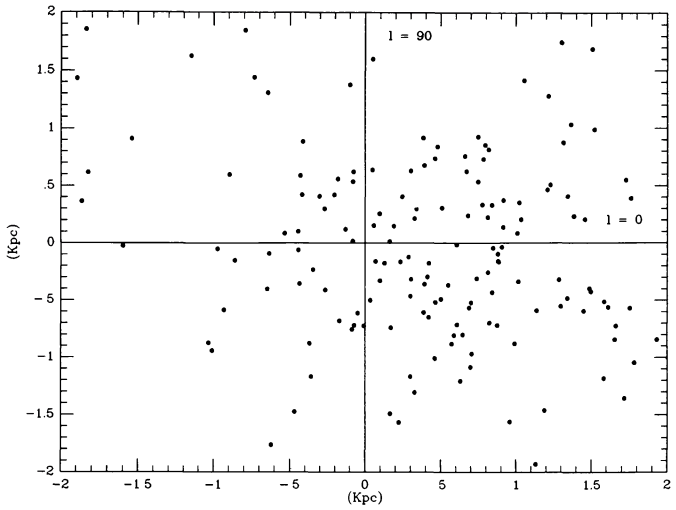

FIG. 6.—The projection onto the Galactic plane of the short-period Miras listed in Table 2.

streaming velocity might be comparable to the gas outflow velocity. Specifically, we may write (Kwan & Linke 1982)

$$v_{st} = v_\infty Q^{1/2}[(L/cv_\infty dM/dt)]^{1/2} , \quad (13)$$

where Q is the ratio of the momentum transfer to the geometric cross section of the grains. The natural definition of a "low" mass-loss rate is when

$$dM/dt \ll L/(cv_\infty) . \quad (14)$$

For stars with $L_4 = 0.5$ and $v_\infty = 5$ km s^{-1}, the mass-loss rate limit characterized by equation (14) is $2 \times 10^{-5}\ M_\odot$ yr^{-1}. In regions with dM/dt much less than this characteristic value, v_{st} may be comparable to v_∞, depending upon Q. For the stars listed in Table 3 where the mass-loss rate is only $\sim$0.01 of that given by the limit in equation (14), we take $v_{st} = v_\infty$. Whether the mean value for v_{st} is actually this large depends upon the relative numbers of small and large grains in the outflow. Here, we use

$$v_{dust} = 2v_\infty . \quad (15)$$

From equations (11) and (15), we derive the mass-loss rates listed in Table 3. With the dust velocity given in this fashion, we find that the mass-loss rates derived from analysis of the CO emission and that derived from analysis of the far-infrared emission usually agree within a factor of 2. It seems that the characteristic mass-loss rate from an intermediate-period Mira is between 1 and $2 \times 10^{-7}\ M_\odot$ yr^{-1}.

4. SHORT-PERIOD MIRAS

4.1. *Spatial Distribution*

We now consider the 211 short-period Miras listed in Table 2, and apply a similar analysis to infer their spatial distribution as we did for the intermediate-period Miras described above. In Figure 6, we display a projection onto the plane of the Milky Way of the short-period Miras listed in Table 2; we find a marked concentration toward the Galactic center. There are 61 stars listed in Table 2 in the longitude zone 330°–30°, and their median distance from the Sun projected onto the Galactic plane is 1500 pc. In the longitude zone 150°–210°, there are 11 stars listed in Table 2 with a median distance from the Sun of 800 pc. Therefore, a variation in Galactocentric radius of $\sim$2300 pc leads to about a factor of 5 change in the surface density of oxygen-rich Miras, indicating a scale length in the Galactic disk of $\sim$1500 pc, a value much smaller than the 4500 and 6500 pc given by Habing (1988) for the "thin disk" and "thick disk" red *IRAS* sources, respectively. However, Habing's (1988) result is not directly comparable to ours since his exponential scale length of the "thin disk" stars pertains to the inner Galaxy and in the neighborhood of the Sun there is a "cutoff" at 1 kpc beyond the Solar circle. Therefore, our result for the short-period Miras resembles Habing's (1988) result that even within $\sim$1 kpc of the Sun there is a marked concentration of these stars toward the Galactic center.

The "cutoff" in the "thin disk" stars losing a large amount of mass found by Habing is a result of his color criteria which effectively excluded most carbon stars from his sample, together with the fact that there is a substantial Galactocentric gradient in the ratio of carbon-rich to oxygen-rich AGB stars (Jura 1990). At the moment, there is no evidence that the rapid decrease in the surface density of short-period Miras as a function of Galactocentric distance is a result in a change in the properties of these stars.

We now determine the exponential scale height described by equation (5). If we assume that all the stars without measured distances are farther from the Sun than the median value, the median distance is 1400 pc, while if we assume that the stars without known distances are randomly distributed, the median distance from the Galactic plane for the short-period Miras is $\sim$1300 pc. We assume that the true value of the me-

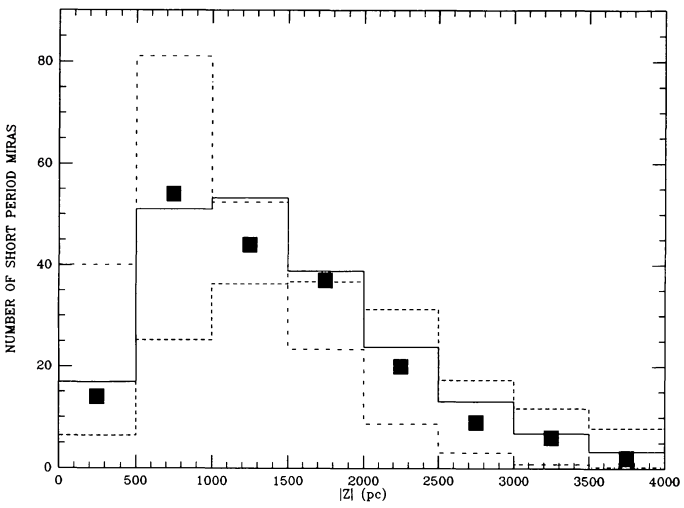

FIG. 7.—A histogram of the distribution of distances from the Galactic plane of the short-period Miras listed in Table 1 compared with the exponential distribution given by eq. (5). The solid curve is for $Z_0 = 500$ pc, our inferred value of the exponential scale height, while the dashed curve is for $Z_0 = 750$ pc, and the dot-dashed curve is for $Z_0 = 330$ pc.

dian is ~1350 pc which corresponds from equation (7) to Z_0 = 500 pc. We find no difference for the exponential scale height of the stars with 200 < P < 300 days and those with 100 < P < 200 days, and so we have not subdivided the short-period Miras into these two different groups. In Figure 7 we display a comparison between models with different values of Z_0 and the data; we find that a model with Z_0 = 500 pc agrees well with the observed distribution. If we use the period K-band luminosity relationship given by equation (1) instead of that given by equation (2), the exponential scale height could be as high as 600 pc. In Appendix A, we argue that our sample of short-period Miras is better than 75% complete to a distance of 2000 pc from the Sun. This distance is sufficiently larger than our inferred value of the exponential scale height of short-period Miras that our estimates of the space density of these stars should be reasonably accurate.

If we restrict our analysis to those stars with $|b| > 60°$ so as not to be as affected by the Galactocentric gradient in the density of stars, we again find a median height of ~1350 pc. Similarly, if we consider separately the hemispheres facing the Galactic center and anticenter, we again find that the median height in each sample is ~1300 pc. No matter how we subdivide the sample, we find essentially the same result for Z_0.

In order to estimate the local space density and surface density projected onto the Galactic plane of the short-period Miras, it is necessary to exclude regions that are so far away that they exhibit substantial changes from the local value. Consequently, we restrict our analysis to the subsample of stars in Table 2 with $|b| > 45°$. In this case, since $N_* = 95$, we find from equations (6) and (7) that n_0 = 60 kpc^{-3} while σ = 60 kpc^{-2}. If the scale height is 600 pc instead of 500 pc, these values for the density and surface density should be n_0 = 35 kpc^{-3} and σ = 40 kpc^{-2}. These values for the surface density are considerably higher than the value of 2.5 kpc^{-2} derived by Habing (1988) for the "thick disk" stars losing a large amount of mass.

As far as we can tell the space distribution of the short-period Miras is better described as a disk rather than a spheroid because there is no evidence for any Galactocentric gradient of the mean distance from the Galactic plane as would be expected for a spheroid.

4.2. *Mass Loss and Metallicity*

In part because of their typically greater distances from the Sun than the intermediate-period Miras, we have less information about the mass-loss rates from the short-period Miras. For example, in the compilation by van der Veen & Rugers (1989), only two oxygen-rich Miras with periods less than 300 days are detected CO sources: GY Aql and R Aql.

It is possible to demonstrate that the short-period Miras are losing substantial amounts of mass from their *IRAS* colors. According to van der Veen & Habing (1988), M stars are losing mass (in their region II), perhaps $10^{-7}\ M_\odot\ \mathrm{yr}^{-1}$, if the *IRAS* colors are such that

$$F_\nu(12\ \mu\mathrm{m})/F_\nu(25\ \mu\mathrm{m}) > 0.33\ . \qquad (16)$$

This relationship indicates the presence of very cool circumstellar material since we expect emission from a photosphere should equal the ratio in the Rayleigh Jeans limit of 0.23. Of the over 150 stars in Table 2 for which both the 12 and 25 μm fluxes are reported in the IRAS Point Source Catalog, over 90% of them satisfy the inequality in equation (16). The remainder show $F_\nu(12\ \mu\mathrm{m})/F_\nu(25\ \mu\mathrm{m}) > 0.30$ and they also are probably losing mass.

Our estimate of the mass-loss rate of $\sim 10^{-7}\ M_\odot\ \mathrm{yr}^{-1}$ from equation (11) is much less than that of $5 \times 10^{-6}\ M_\odot\ \mathrm{yr}^{-1}$ given by Frogel & Elias (1988) for Miras with periods near 200 days in globular clusters. However, there are numerical errors in their analysis. We find that the coefficient in front of their equation (6) should be 8.8×10^7 instead of 8.3×10^{-7}. In their notation, we therefore rewrite their equation (6) to derive

$$\kappa dM/dt = 1.1 \times 10^{-8}(f_\nu D^2) v \lambda^{1/2} R_0^{-1} T_0^{-5/2} [I(x)]^{-1}\ , \qquad (17)$$

where κ is the opacity of the gas and dust together (cm^2 g^{-1}), dM/dt is the mass-loss rate of gas ($10^{-10}\ M_\odot\ \mathrm{yr}^{-1}$), f_ν the observed flux (ergs cm^{-2} s^{-1} Hz^{-1}) at wavelength λ (μm), v the outflow velocity (km s^{-1}), D the distance (cm), and R_0 the radius of the star ($R_\odot$), T_0 the effective temperature of the star (K) and $I(x)$ an integral given by Frogel & Elias (1988) which is close to unity. For the Mira star 47 Tuc VI, the star with the

TABLE 4

SUMMARY PROPERTIES OF AGB STARS

Type of Star	Z_0 (pc)	σ (kpc^{-2})	n_0 (kpc^{-3})	R_0 (kpc)	M_{MS}[a] ($M_\odot$)	References
All carbon	200	40	100	>5	1.5	1, 2
"Very dusty carbon"	~200	~10	30	>5	1.5	3, 4
S-type	200	12	30	?	1.5	5
Oxygen-rich Mira $300 < P < 400$ days	240	100	210	~3.5	1.1	6
Oxygen-rich Mira $P < 300$ days	500–600	40–60	35–60	1.5?	<1.1	6
"Very dusty" oxygen	~200	10–15	30	~4	~1.2	4, 7

[a] M_{MS} refers to the typical mass of the main-sequence progenitor. The symbols are defined in eqs. (5) and (8).

REFERENCES.—(1) Claussen et al. 1987; (2) Jura, Joyce, & Kleinmann 1989; (3) Jura & Kleinmann 1989; (4) Jura & Kleinmann 1990a; (5) Jura 1988; (6) this paper; (7) Habing 1988.

highest mass-loss rate in their Table 1, Frogel & Elias (1988) estimated a loss rate of $\sim 10^{-5}\ M_\odot\ \mathrm{yr}^{-1}$ since the flux at 10 μm is 0.4 Jy and the distance can be taken as 4200 pc. However, with $v = 10\ \mathrm{km\ s}^{-1}$, $T_0 = 3300$ K, $R_0 = 200\ R_\odot$ and $\kappa(10\ \mu\mathrm{m}) = 12\ \mathrm{cm}^2\ \mathrm{g}^{-1}$ for a mixture of gas and dust representative of the interstellar medium (Draine & Lee 1984; Spitzer 1978), we estimate from equation (17), our revision of their formalism, that $dM/dt = 1.6 \times 10^{-8}\ M_\odot\ \mathrm{yr}^{-1}$. If we used equation (11) with the same parameters for 47 Tuc VI and extrapolated the observed flux at 10 to 60 μm with the result that $F_\nu(60\ \mu\mathrm{m}) = 0.03$ Jy because it varies as $\nu^{1.5}$ (as would be predicted in the model of Frogel & Elias 1988 or Sopka et al. 1985), we find that $dM/dt = 3.2 \times 10^{-8}\ M_\odot\ \mathrm{yr}^{-1}$. The factor of 2 difference in mass-loss rates between equations (11) and (17) comes from different assumptions about the dust to gas ratio and emissivity of the dust. Even if dust to gas ratio in the outflows from these stars is one-third of that in local Miras, it is likely that the mass-loss rates are less than $10^{-7}\ M_\odot\ \mathrm{yr}^{-1}$.

Because the short-period Miras are derived from a different population than the intermediate-period Miras, we cannot assume that they have the same metallicity. Although a detailed photospheric analysis would be more accurate, we can argue from the presence of significant amounts of circumstellar dust that the metallicity of the short-period Miras is not very much lower than solar. That is, because both short- and intermediate-period Miras have similar values for $F_\nu(12\ \mu\mathrm{m})/F_\nu(25\ \mu\mathrm{m})$, it seems likely that they have comparable amounts of circumstellar dust. Because the dust typically carries half of the material heavier than helium in the outflows from AGB stars (see, for example, Jura 1990), this implies that the mean metallicity of the short-period Miras is at least one-third of the mean metallicity of the intermediate-period Miras. This result is roughly consistent with the finding that only globular clusters with metallicities greater than 0.1 of the solar value contain Mira variables (Frogel & Elias 1988; Lloyd Evans 1989).

5. DISCUSSION

In Table 4, we summarize our estimates for different kinds of AGB stars. As found previously in kinematic studies, the short- and intermediate-period oxygen-rich Miras evolve from different progenitor populations. Although less certain, it seems possible that the carbon stars and the intermediate-period Miras also arise from different populations.

Wood & Cahn (1977) proposed a model of the space distribution of all Miras with an exponential scale height of 310 pc, a surface density of 150 kpc^{-2} and a space density in the plane of the Milky Way of 245 kpc^{-3}. If we combined the intermediate- and short-period oxygen-rich Miras together, we would get approximately these results. However, it is important to separate the different kinds of Miras.

The standard picture is that oxygen-rich Miras are a phase during the AGB evolution of that are initially near 1 $M_\odot$; our results are consistent with this picture. The spatial distribution around the Galactic plane of the intermediate-period Miras can be well represented by an exponential with a scale height of $\sim$240 pc, in agreement with that of main sequence stars of $\sim 1.1\ M_\odot$.

We find that the oxygen-rich Miras with $P < 400$ days typically lose $2 \times 10^{-7}\ M_\odot\ \mathrm{yr}^{-1}$. Because we estimate a duration of this phase of $\sim 2 \times 10^5$ yr, we propose that during the Mira phase, these stars lose less than $\sim 0.1\ M_\odot$. During the course of their evolution from 1.1 $M_\odot$ stars on the main-sequence to white dwarfs of 0.6 $M_\odot$, these stars must lose 0.5 $M_\odot$. Because they lose 0.1 $M_\odot$ or less during the Mira phase, this implies that most of their mass loss occurs during some other phase(s) of their evolution.

Jura & Kleinmann (1989) have found that for carbon stars, the total return into the interstellar medium is dominated by relatively few objects of intense mass loss (characteristically $10^{-5}\ M_\odot\ \mathrm{yr}^{-1}$) rather than the more common carbon stars with lower mass rates (characteristically $10^{-7}\ M_\odot\ \mathrm{yr}^{-1}$). We suggest that a similar phenomenon occurs for the intermediate-period Miras. Jura & Kleinmann (1989) estimated a surface density of "very dusty" oxygen-rich stars in the solar neighborhood of $\sim$10–15 kpc^{-2}, about one-eighth of the surface density derived here for the intermediate-period Miras. Because the "very dusty" stars lose mass at $\sim 10^{-5}\ M_\odot\ \mathrm{yr}^{-1}$ or 100 times the rate of the optically bright Miras discussed here, they dominate the net loss of mass by these stars. Because only one of the "very dusty" oxygen-rich stars listed by Jura & Kleinmann (1989), V342 Sgr, has a pulsational period less than 400 days, we suspect that the length of a Mira's period increases during the phase of intense mass loss. Since we have less knowledge about the short-period Miras; we cannot demonstrate that they undergo a phase of intense mass loss.

In agreement with the previous kinematic studies (Feast 1963), we find that the space distribution of the short-period Miras ($P < 300$ days) is quite distinctive from that of the intermediate-period Miras. The space distribution around the Galactic plane of the short-period Miras can be modeled as an exponential with a scale height of between 500 and 600 pc. Their main-sequence progenitors are not enumerated in the single-component models of local dwarfs by Miller & Scalo (1979) or Bahcall (1984). Instead, we find *qualitative* agreement with the picture of Gilmore & Reid (1983) and Kuijken & Gilmore (1989) that there must be an additional subpopulation of dwarfs with masses 1.1 $M_\odot$ or less that have an exponential scale height much larger than 300 pc. Feast (1988) also has noted that the short-period Miras can be used to trace out the space distribution of the "thick disk" stars. However, the exponential scale we derive for the short-period Miras of $\sim$500 or 600 pc is much less than the value of 1000 pc or more proposed by Gilmore & Reid (1983) and Kuijken & Gilmore (1989) for the "thick disk" stars.

Habing (1988) estimated that the "thick disk" stars losing a large amount of mass might have an exponential scale height between 600 and 1200 pc; he could not distinguish between these two possibilities. Because the short-period Miras are so luminous, they offer one of the most accurate ways to measure the exponential scale height of these very old stars. Our results would favor a scale height for these "thick disk" stars of closer to 600 pc.

As summarized in Table 4, the space density of short-period Miras is at least one-eighth of the space density of the intermediate-period Miras. Although we do not know the relative lifetimes of these two different kinds of stars, we therefore require that a substantial fraction of the local main-sequence stars with masses 1.1 $M_\odot$ or less are progenitors to the short-period Miras. This argument is qualitatively consistent with the picture of

Gilmore & Reid (1983) and Kuijken & Gilmore (1989) that somewhere between 2% and 4% of the local dwarfs with masses 1.1 $M_\odot$ or less belong to a subpopulation with an exponential scale height much greater than the 300 pc that is characteristic of most of the local main-sequence stars.

Finally, as noted in § 1, Winget et al. (1987) and Liebert et al. (1988) have found about a factor of 10 fewer white dwarfs with luminosities less than 10^{-4} $L_\odot$ than predicted by standard models. Because the exponential scale height of the short-period Miras is only about a factor of 2 larger than the exponential scale height of the intermediate-period Miras, the absence of the low-luminosity white dwarfs does not seem to be merely a consequence of a greater mean distance of the oldest stars from the Galactic plane (Iben & Tutukov 1984). If, however, the masses of the progenitors of the short-period Miras are significantly less than 1.0 $M_\odot$, there must be a substantial number of stars older than 10^{10} yr in the solar neighborhood. The existence of such a subpopulation would severely challenge the current interpretation of the white dwarf luminosity function; it would suggest an age for the disk significantly greater than 8 billion yr.

6. CONCLUSIONS

1. The spatial distribution of the intermediate period Miras ($300 < P < 400$ days) about the Galactic plane can be well modeled by an exponential with a scale height of ~240 pc. This scale height indicates that they are descended from main-sequence dwarfs of typically ~1.1 $M_\odot$. We estimate that there are ~210 kpc^{-3} intermediate-period Miras with a surface density projected onto the Galactic plane of ~100 kpc^{-2}. The lifetime of the Mira phase is $\sim 2 \times 10^5$ yr. Because the Miras typically are losing 2×10^{-7} $M_\odot$ yr^{-1}, they lose 0.1 $M_\odot$ or less during the Mira phase. This mass loss is small compared to the total of 0.5 $M_\odot$ that the star loses before it becomes a white dwarf.

2. The spatial distribution of the short-period Miras ($P <$ 300 days) is well characterized by an exponential scale height of between 500 and 600 pc above the Galactic plane. This scale height is greater than that of the bulk of the disk population of stars; the short-period Miras must be descended from a subpopulation of main-sequence dwarfs with masses ≤ 1.1 $M_\odot$ or less that are not included in the standard single-component models that have an exponential scale height of ~300 pc. The number density of the short-period Miras is between 35 and 60 kpc^{-3}. Nearly all the short-period Miras have circumstellar dust; this implies that the short-period Miras have metallicities of at least one-third solar.

M. J.'s work has been partly supported by NASA; S. G. has been supported by AFOSR grant 88-0070. We thank S. Tremaine and P. Wood for helpful comments. The referee, M. Feast, provided a very thorough and thoughtful scrutiny of this manuscript.

APPENDIX A

Here we discuss the completeness of our listing of Miras at $|b| > 30°$ in Tables 1 and 2. Because the depth of the optical surveys of the sky is unknown, we evaluate the counts of Miras in the TMSS and in *IRAS*.

1. We consider all the stars in the TMSS that have $|b| > 30°$.

2. Furthermore, as demonstrated in Figure 3, Miras typically have substantial amounts of circumstellar dust emission, and we only consider stars with $F_\nu(12\ \mu\text{m})/F_\nu(2\ \mu\text{m}) > 0.2$.

Most of the stars satisfying criterion 1 in the TMSS are also listed in Kholopov et al. (1985) and their optical variations are classified. There are only 21 stars [-30013(v), 20023[=SAO 74694], -20019(v), 20032[=SAO 92697], 20032[=SAO 92697], -20062(v), 60184, 40206[=SAO 42901], 20216[=SAO 98945], -10245, -20226[=SAO 179810], 30241, -20285, -20290, 00270, 00281, -30433, -10573[=SAO 164760], 10510(v), 10523, 10525(v)], which satisfy criteria 1 and 2 and which might possibly be Miras because they are not classified in the catalog of Kholopov et al. (1985). The five stars that are variable at K in the TMSS are designated by *v*. Therefore, only 24% of these 21 unclassified stars are known to be variable at K; this is in contrast to the ~75% of the Miras in the TMSS which display variability in that catalog. Also, of these 21 stars, seven have identifications in the Smithsonian Astrophysical Observatory catalog (denoted by SAO) and these stars that are sufficiently bright, $m_V < 10.0$ mag, that they are probably not unknown Miras. One star, -30013 = AD Scl, is reported by Kholopov et al. (1985) to display a range in optical variation of 2.5 mag but no period is given.

Because of the lack of variability of most of the unidentified stars, we think that Tables 1 and 2 are missing at most 12 stars that are brighter than $m_K = 3.0$ mag and that lie in the zone of declination covered by the TMSS. Consequently, if the mean period of the short-period Miras is ~200 days, then this sample is nearly complete to a distance of ~900 pc and, similarly, the list of intermediate-period Miras (assuming a typical mean period of 350 days) is nearly complete to ~1300 pc. If we assume that at most half of the 12 stars with unknown properties of their optical variation are intermediate-period Miras, and since the TMSS covered ~75% of the sky, we estimate that our Table 1 misses at most eight Miras in the same volume where we know that there are 80 Miras. Therefore, we think that our catalog of intermediate-period Miras in Table 1 is complete to better than 90% to a distance of 1300 pc from the Sun.

In order to evaluate the completeness of the listing of the short-period Miras, we consider the objects in the *IRAS* catalog at high Galactic latitudes. Hacking et al. (1985) list all the objects with $F_\nu(12\ \mu\text{m}) \geq 28$ Jy and $|b| > 30°$. However, this search is not deep enough for our purposes. In order to evaluate the completeness of the sky, we restrict our analysis to the zone with $|b| > 60°$ in the declination zone covered by the TMSS. We have compiled all the objects in this zone with $F_\nu(12\ \mu\text{m}) > 2$ Jy and $F_\nu(25\ \mu\text{m})/F_\nu(12\ \mu\text{m}) \geq 0.33$ as is characteristic of Miras. For a mean period of 200 days, this corresponds to a search volume of nearly 2000 pc (see eq. [3]). We also omit all stars that are listed in the TMSS or have been studied in the GCVS. There are 14 such sources (01181 −

0840[=SAO 129240], 01295 − 1704, 01333 − 1137, 01371 − 0809, 01556 − 2643[=SAO 167437], 02296 − 1944, 02324 − 2106, 11554 + 5252, 11049 + 3845, 12321 + 0002, 12462 + 0738, 12480 + 1337, 14545 + 2742, 14588 + 3134[=SAO 64464]). Because they are bright at optical wavelengths, the SAO stars are not likely to be unidentified Miras. Some of the remaining 11 of these sources may prove to be short-period Miras. In this same region of the sky, we have identified in Table 2, 33 short-period Miras, and therefore, we think that Table 2 is more than 75% complete to a distance of 2000 pc from the Sun.

APPENDIX B

The shape of the optical light curve of a Mira can be characterized by the asymmetry parameter, f, which is the percentage of the time spent from minimum to maximum light compared to the star's period. Bowers (1975) showed that oxygen-rich Miras were more likely to be detected as OH masers if f were smaller than average. Vardya, de Jong, & Willems (1986) found that Miras with smaller values of f were more likely to display the silicate emission feature at 9.7 μm in the LRS spectra obtained with the *IRAS* satellite. These two results can be largely understood if the Miras with smaller values of f have greater mass-loss rates (Onaka, de Jong, & Willems 1989a,b; Vardya 1989).

Our nearly complete sample allows us to extend previous studies by asking whether different period Miras might behave differently; almost all the Miras in the previous samples have $P > 300$ days. Here, we examine the possibility that the short- and intermediate-period Miras exhibit different behaviors with regard to f.

In Tables 1 and 2, we list all the values of f that are available from the GCVS; ~50% of the stars have reported values of this quantity. Ignoring the apparently anomalous values for VV Her ($f = 2$) and RU Ari ($f = 4$), we find that the average value of f for the short-period Miras is 45.2 while for the intermediate-period Miras, the average value of f is 42.9. Because there is an inverse correlation between the amount of circumstellar dust and the value of f (Onaka et al. 1989a), this result is consistent with equations (3) and (4). An inverse correlation of the average value of f with the period of a Mira is also shown in Table 1 of Bowers (1975).

It is also possible to demonstrate that the anticorrelation of mass-loss rate with f only pertains to stars with $P > 300$ days. (This result is suggested in Table 1 of Bowers 1975, but because he had only three stars with $P < 300$ days that were detected as OH emitters, the sample was too small to use to determine if the f-dependence of the mass-loss rate is a function of period). In Figure 8, we display a plot of $F_\nu(60\ \mu\text{m})/F_\nu(2\ \mu\text{m})$ for all the intermediate-period Miras in Table 1 except VV Her and RU Ari for which (1) the flux at 2.2 μm is measured (and not extrapolated from eq. [4]) and (2) the 60 μm flux is detected in the *IRAS* Point Source Catalog. This plot is similar to Figure 2 in Onaka et al. (1989a) except that we plot the flux at 2.2 μm rather than 3.5 μm. We find an inverse correlation of f with the ratio of $F_\nu(60\ \mu\text{m})/F_\nu(2\ \mu\text{m})$ as expected from previous studies. In Figure 9, we plot the same quantity for all the short-period Miras in Table 2 for which (1) we have a measured flux at 2.2 μm not extrapolated from equation (4) and (2) the 60 μm flux is detected in the *IRAS* Point Source Catalog. Figure 9 does not display the same anticorrelation between f and inferred mass loss as shown in Figure 9.

We conclude that as implied in the analysis by Bowers (1975): (1) the average value of f is greater for short-period Miras than for intermediate- and long-period Miras and (2) the anticorrelation of mass-loss rate with f found for intermediate-period Miras does not pertain to short-period Miras. Even though progress has been made (Bowen & Willson 1991), we still do not have a full understanding about the relationships between the shocks produced by the Mira variability, the formation of circumstellar dust grains, and the mass loss from these stars.

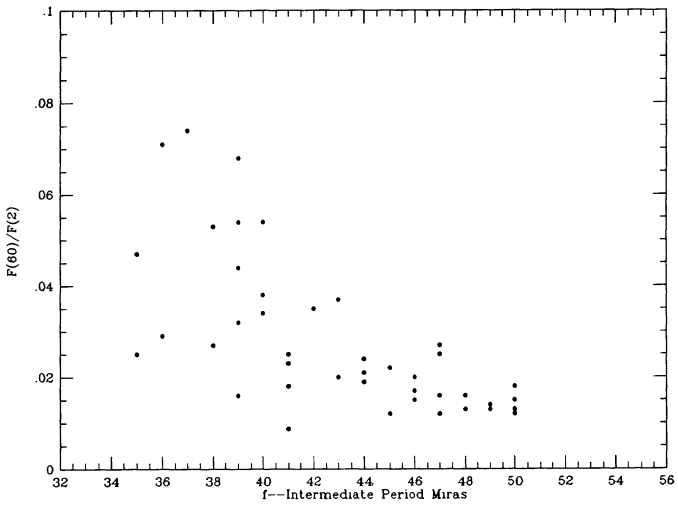

FIG. 8.—A plot of f vs. $F_\nu(60\ \mu\text{m})/F_\nu(2\ \mu\text{m})$ for the intermediate-period Miras in Table 1.

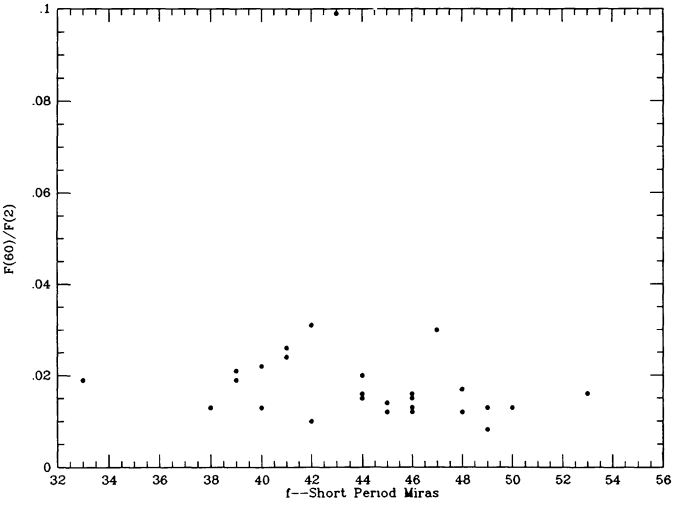

FIG. 9.—The same as Fig. 8 for the short-period Miras in Table 2. The anomalous point at $f = 43$ is R Cet, a star which probably has a relatively high mass loss for its short period because it is detected as an OH maser (Sivagnanam et al. 1988).

REFERENCES

Bahcall, J. N. 1984, ApJ, 287, 926
Beckwith, S., Evans, N. J., Becklin, E. E., & Neugebauer, G. 1976, ApJ, 208, 390
Blaauw, A. 1965, in Galactic Structure, ed. A. Blaauw & M. Schmidt (Univ. of Chicago Press), 435
Bothun, G., Elias, J. H., MacAlpine, G., Matthews, K., Mould, J. R., Neugebauer, G., & Reid, I. N. 1991, AJ, 101, 2220
Bowen, G. H., & Willson, L. A. 1991, ApJ, 375, L53
Bowers, P. F. 1975, A&A, 39, 473
Bujarrabal, V., Gómez-González, J., & Planesas, P. 1989, A&A, 219, 256
Cahn, J. H., & Wyatt, S. P. 1976, ApJ, 210, 508
Catchpole, R. M., Robertson, B. S. C., Lloyd Evans, T. H. H., Feast, M. W., Glass, I. S., & Carter, B. S. 1979, South Africa Astron. Obs. Circ., 1, 61
Claussen, M. J., Kleinmann, S. G., Joyce, R. R., & Jura, M. 1987, ApJS, 65, 385
Draine, B. T., & Lee, H. M. 1984, ApJ, 285, 89
Feast, M. W. 1963, MNRAS, 125, 367
———. 1989, in IAU Colloquium 111, The Use of Pulsating Stars in Fundamental Problems of Astronomy, ed. E. G. Schmidt (Cambridge Univ. Press), 205
Feast, M. W., Glass, I. S., Whitelock, P. A., & Catchpole, R. M. 1989, MNRAS, 241, 375
Frogel, J. A., & Elias, J. H. 1988, ApJ, 324, 823
Gezari, D. Y., Schmitz, M., & Mead, J. M. 1987, Catalog of Infrared Observations, NASA RP 1196
Gilmore, G., & Reid, N. 1983, MNRAS, 202, 1025
Habing, H. J. 1988, A&A, 200, 40
———. 1990, in From Miras to Planetary Nebulae: Which Path for Stellar Evolution?, ed. M. O. Mennessier & A. Omont (Gif sur Yvette: Editions Frontières), 16
Hacking, P., et al. 1985, PASP, 97, 616
Harmon, R., & Gilmore, G. 1988, MNRAS, 235, 1025
Hughes, S. M. G., & Wood, P. A. 1990, AJ, 99, 784
Iben, I., & Tutukov, A. V. 1984, ApJ, 282, 615
IRAS Point Source Catalog 1985, Joint *IRAS* Science Working Group (Washington, DC: US GPO)
Jura, M. 1987, ApJ, 313, 743
———. 1988, ApJS, 66, 33
———. 1990, in From Miras to Planetary Nebulae: Which Path for Stellar Evolution?, ed. M. O. Mennessier & A. Omont (Gif sur Yvette: Editions Frontières), 41
Jura, M., Joyce, R. R., & Kleinmann, S. G. 1989, ApJ, 336, 924
Jura, M., & Kleinmann, S. G. 1989, ApJ, 341, 359
———. 1990a, ApJ, 364, 663
———. 1990b, ApJS, 73, 769
Kenyon, S. J., & Gallagher, J. S. 1983, AJ, 88, 666
Kholopov, P. N., et al. 1985, General Catalogue of Variable Stars (4th ed., Moscow: Moscow Pub. House)
Kuijken, K., & Gilmore, G. 1989, MNRAS, 239, 605
Kwan, J., & Linke, R. A. 1982, ApJ, 254, 587
Liebert, J., Dahn, C. C., & Monet, D. G. 1988, ApJ, 332, 891
Little, S. J., Little-Marenin, I. R., & Bauer, W. H. 1987, AJ, 94, 981
Lloyd Evans, T. 1989, in Evolution of Peculiar Red Giants, IAU Colloquium 106, ed. H. R. Johnson & B. Zuckerman (Cambridge Univ. Press), 241
Lockwood, G. W., & Wing, R. W. 1971, ApJ, 169, 63
Lynds, B. T. 1962, ApJS, 7, 1
Magnani, L., Lada, E. A., & Blitz, L. 1986, ApJ, 301, 395
Miller, G. E., & Scalo, J. M. 1970, ApJS, 41, 513
Neugebauer, G., & Leighton, R. B. 1969, Two Micron Sky Survey, NASA SP-3047
Onaka, T., de Jong, T., & Willems, F. J. 1989a, A&A, 218, 169
———. 1989b, A&AS, 81, 261
Plaut, L. 1965, in Galactic Structure, ed. A. Blaauw & M. Schmidt (Univ. of Chicago Press), 267
Reid, N., Glass, I. S., & Catchpole, R. M. 1988, MNRAS, 232, 53
Sivagnanam, P., Le Squeren, A. M., & Foy, F. 1988, A&A, 206, 285
Sopka, R. J., Hildebrand, R., Jaffe, D. T., Gatley, I., Roellig, T., Werner, M., Jura, M., & Zuckerman, B. 1985, ApJ, 294, 242
Spitzer, L. 1978, Physical Processes in the Interstellar Medium (New York: Wiley)
van der Veen, W. E. C. J., & Habing, H. J. 1988, A&A, 194, 125
van der Veen, W. E. C. J., & Rugers, M. 1989, A&A, 226, 183
Vardya, M. S. 1989, A&A, 209, 165
Vardya, M. S., de Jong, T., & Willems, F. J. 1986, ApJ, 304, L29
Weidemann, V. 1990, ARA&A, 28, 103
Whitelock, P., Feast, M., & Catchpole, R. 1991a, MNRAS, 248, 276
Whitelock, P., Feast, M. W., Catchpole, R. M., Carter, B. S., & Roberts, G. 1983, MNRAS, 203, 351
Whitelock, P. A., Menzies, J. W., Catchpole, R. M., Feast, M. W., Roberts, G., & Marang, F. 1991b, MNRAS, 250, 638
Winget, D. E., Hansen, C. J., Liebert, J., Van Horn, H. M., Fontaine, G., Nather, R. E., Kepler, S. O., & Lamb, D. Q. 1987, ApJ, 315, L77
Wood, P. R. 1990, in From Miras to Planetary Nebulae: Which Path for Stellar Evolution?, ed. M. O. Mennessier & A. Omont (Gif sur Yvette: Editions Frontières), 67
Wood, P. R., & Cahn, J. H. 1977, ApJ, 211, 499
Wyatt, S. P., & Cahn, J. H. 1983, ApJ, 275, 225
Zuckerman, B., & Aller, L. H. 1986, ApJ, 301, 772